Vessel Enhancement in 2D Angiographic Images

Sahla Bouattour and Dietrich Paulus

Institute of Computational Visualistics,
University of Koblenz-Landau, Germany
bouattour@uni-koblenz.de
http://www.uni-koblenz.de/agas

Abstract. In this paper we *extend* the Frangi filter[1] to recognize edges and do not enhance them. We give a theoretical framework for *optimal scale selection* and *choice of the free parameters*. We discuss *discretization* details concerning especially the discrete kernel used for building the scale-space and the choice of discrete scales. We present several experiments on phantom data to objectively and *quantitatively* compare and judge the filters. Experiments on real coronary angiograms enhance the improvement reached by the integration of the edge indicator.

Key words: Vessel enhancement, multiscale analysis, phantom evaluation

1 Introduction

In 2D coronary angiograms, vessels appear as curvilinear tubular structures having different widths. To recover the geometric structure, it is common to analyze the local partial derivatives of second order and build differential operators based on the sign and values of eigenvalues[1–3]. To recover the different widths, it is necessary to build operator answers at different levels of scales and to combine them[4]. The goal of vessel enhancement is to enhance *Just* the vessels and reduce noise especially in the background. It is important that the operations performed preserve the quantitative measures such as width of the vessel, and that the points with strongest response lie on the centerlines.

In this paper we extend the method proposed by Frangi et. al[1] to recognize edges and do not enhance them. Furthermore we perform a theoretical multiscale analysis to give theoretical values or bounds for the filter free parameters. Section 2 presents the new method. Section 3 discusses discretization details to get a proper realization. Section 4 presents experimental results, also on a phantom image. Finally Section 5 concludes this work.

2 Method

Given a continuous two-dimensional image $I(\bar{\boldsymbol{x}})$ ($\bar{\boldsymbol{x}} \in \mathrm{IR}^2$) that is observed at a scale $t \in \mathrm{IR}$, the Frangi et al. enhancement operator for bright vessels [1] is conceived as a filter with filter response:

$$r(\bar{\boldsymbol{x}}, t, \beta_1, \beta_2) = \begin{cases} 0 & \text{if } \lambda_2(\bar{\boldsymbol{x}}, t) > 0, \\ \exp(\frac{-\mathcal{R}_B{}^2(\bar{\boldsymbol{x}},t)}{2\beta_1^2})(1-\exp(-\frac{\mathcal{S}^2(\bar{\boldsymbol{x}},t)}{2\beta_2^2})), & \end{cases} \tag{1}$$

where $\lambda_1(\bar{\boldsymbol{x}},t)$ and $\lambda_2(\bar{\boldsymbol{x}},t)$ are the eigenvalues of the local Hessian computed at $\bar{\boldsymbol{x}}$ at scale t, such that $|\lambda_1(\bar{\boldsymbol{x}},t)| < |\lambda_2(\bar{\boldsymbol{x}},t)|$. The blobness measure $\mathcal{R}_{\mathcal{B}}(\bar{\boldsymbol{x}},t) = \frac{\lambda_1(\bar{\boldsymbol{x}},t)}{\lambda_2(\bar{\boldsymbol{x}},t)}$ measures the deviation from a blob by accounting for the eccentricity of the second order ellipse. $\mathcal{R}_{\mathcal{B}}(\bar{\boldsymbol{x}},t)$ cannot distinguish between a line and an edge. The structureness measure $\mathcal{S}(\bar{\boldsymbol{x}},t) = \sqrt{\lambda_1^2(\bar{\boldsymbol{x}},t) + \lambda_2^2(\bar{\boldsymbol{x}},t)}$ is the norm of the Hessian and is computed to distinguish between background and vessels. The parameters β_1 and β_2 tune the sensitivity of the filter to deviations in $\mathcal{R}_{\mathcal{B}}(\bar{\boldsymbol{x}},t)$ and $S(\bar{\boldsymbol{x}},t)$.

In order to distinguish between line and edge structures we propose to additionally integrate an edge indicator. Lorenz [3] proposed the following – here slightly modified – indicator:

$$E(\bar{\boldsymbol{x}},t) = \frac{|\nabla L(\bar{\boldsymbol{x}},t)|}{\sqrt{t}\lambda_2(\bar{\boldsymbol{x}},t)} \tag{2}$$

where $|\nabla L(\bar{\boldsymbol{x}},t)|$ is the local gradient magnitude at a point $\bar{\boldsymbol{x}}$ observed at scale t. At an edge both the gradient and λ_2 will be strong in magnitude. Within a vessel, just λ_2 will be big in magnitude. So it is expected that the value of E decreases within a vessel. We integrate the edge indicator within the Frangi filter as in eq. 3

$$r(\bar{\boldsymbol{x}},t,\beta_1,\beta_2) = \begin{cases} 0 & \text{if } \lambda_2 > 0, \\ \exp(\frac{-{\mathcal{R}_{\mathcal{B}}}^2(\bar{\boldsymbol{x}},t)}{2\beta_1^2})(1-\exp(-\frac{\mathcal{S}^2(\bar{\boldsymbol{x}},t)}{2\beta_2^2}))\exp(-|E(\bar{\boldsymbol{x}},t)|) \end{cases} \tag{3}$$

The continuous image observed at scale $t \neq 0$ is given by the convolution 4

$$L(\bar{\boldsymbol{x}},t) = I(\bar{\boldsymbol{x}}) * G(\bar{\boldsymbol{x}},t), \tag{4}$$

where $G(\bar{\boldsymbol{x}},t)$ is the Gaussian kernel with standard deviation $\sigma = \sqrt{t}$. Both the first order and the second order derivatives are computed by convolving the image $I(\bar{\boldsymbol{x}})$ with respectively the first and second derivatives of the Gaussian. The scale t is continuous and positive. $L(\bar{\boldsymbol{x}},t)$ is called the *scale-space* of the image $I(\bar{\boldsymbol{x}})$ [4].

As vessels appear in images with different widths, the application of filter 3 at different scales is necessary. Lindeberg proposed to use γ-parameterized normalized Gaussian derivatives: $\left(\frac{\partial G(\bar{\boldsymbol{x}},t)}{\partial \bar{\boldsymbol{x}}}\right)^{\gamma-\text{norm}} = t^{\frac{\gamma}{2}}\frac{\partial G(\bar{\boldsymbol{x}},t)}{\partial \bar{\boldsymbol{x}}}$, to get filter answers which are comparable for different scales. Using these operators, it can be easily shown that the normalization is directly transfused on the eigenvalues: $\lambda^{\gamma-\text{norm}}(\bar{\boldsymbol{x}},t) = t^{\frac{\gamma}{2}}\lambda(\bar{\boldsymbol{x}},t)$. Both the blobness measure ${\mathcal{R}_{\mathcal{B}}}^{\gamma-\text{norm}}(\bar{\boldsymbol{x}},t)$ and the edge indicator $E^{\gamma-\text{norm}}(\bar{\boldsymbol{x}},t)$ do not change. Just the structureness measure $\mathcal{S}^{\gamma-\text{norm}}(\bar{\boldsymbol{x}},t) = t^{\frac{\gamma}{2}}\mathcal{S}$ should be normalized. The normalized filter response is then given by eq. 5:

$$r^{\gamma-\text{norm}}(\bar{\boldsymbol{x}},t,\beta_1,\beta_2,\gamma) = \begin{cases} 0 & \text{if } \lambda_2 > 0, \\ \exp(\frac{-{\mathcal{R}_{\mathcal{B}}}^2(\bar{\boldsymbol{x}},t)}{2\beta_1^2})(1-\exp(-\frac{t^\gamma\mathcal{S}^2(\bar{\boldsymbol{x}},t)}{2\beta_2^2}))\exp(-|E(\bar{\boldsymbol{x}},t)|) \end{cases} \tag{5}$$

where $\mathcal{R}_{\mathcal{B}}(\bar{\boldsymbol{x}},t), \mathcal{S}(\bar{\boldsymbol{x}},t)$ and $E(\bar{\boldsymbol{x}},t)$ are computed based on the non-normalized Gaussian derivatives.

The multi-scale responses are combined by maximization:

$$R(\bar{\boldsymbol{x}},\beta_1,\beta_2,\gamma) = \max_t \left(r^{\gamma-\text{norm}}(\bar{\boldsymbol{x}},t,\beta_1,\beta_2,\gamma)\right) \tag{6}$$

Optimal Scale Selection and Choice of γ: In order to specify γ we assume a simple mathematical model for a 2D vessel with Gaussian profile, which is centered in the origin and parallel to the y-axis: $I_0(\bar{\boldsymbol{x}}) = G(\bar{\boldsymbol{x}}, t_0) = \frac{1}{\sqrt{2\pi t_0}} \exp\left(\frac{-x^2}{2t_0}\right) = G(x, t_0)$. The scale-space of $I_0(\bar{\boldsymbol{x}})$ is $L(\bar{\boldsymbol{x}}, t) = I_0(\bar{\boldsymbol{x}}) * G(\bar{\boldsymbol{x}}, t) = G(x, t_0 + t)$ for each value of y. The eigenvalues of the Hessian are $\lambda_1(\bar{\boldsymbol{x}}, t) = 0$ and $\lambda_2(\bar{\boldsymbol{x}}, t) = \frac{\partial^2 L(\bar{\boldsymbol{x}}, t)}{\partial x^2}$. Within the vessel we have $|x| < \sqrt{t_0}$, i.e λ_2 is negative. It follows $|\lambda_1(\bar{\boldsymbol{x}}, t)| < |\lambda_2(\bar{\boldsymbol{x}}, t)|$. The blobness measure $\mathcal{R}_{\mathcal{B}}(\bar{\boldsymbol{x}}, t) = 0$. The structureness measure $\mathcal{S}(\bar{\boldsymbol{x}}, t) = |\lambda_2(\bar{\boldsymbol{x}}, t)|$ and the edge indicator $E(\bar{\boldsymbol{x}}, t) = \frac{|-x|(t+t_0)}{\sqrt{t}(x^2-(t+t_0))}$.

The maximal filter response is expected in the middle of the vessel. At $x = 0$ we have $\mathcal{S}(\mathbf{0}, t) = -\frac{1}{\sqrt{2\pi}(t+t_0)^{\frac{3}{2}}}$ and $E(\mathbf{0}, t) = 0$. The normalized filter response becomes:

$$r^{\gamma-\mathrm{norm}}(\mathbf{0}, t, \beta_1, \beta_2, \gamma) = 1 - \exp\left(-\frac{t^\gamma}{4\pi\beta_2^2(t+t_0)^3}\right) \tag{7}$$

The scale for which this entity is maximal is given by:

$$\frac{\partial r^{\gamma-\mathrm{norm}}(\mathbf{0}, t_{\mathrm{opt}}, \beta_1, \beta_2, \gamma)}{\partial t} \stackrel{!}{=} 0 \longrightarrow t_{\mathrm{opt}} = \frac{\gamma}{3-\gamma} t_0 \tag{8}$$

If we want to have $t_{\mathrm{opt}} = t_0$ we choose $\gamma = \frac{3}{2}$.

It should be mentioned that a different ideal model could lead to another value of γ. The factor γ defines a proportionality between the optimal scale and the characteristic parameter of the assumed model. The later is here assumed to be the standard deviation. The real physical length of the corresponding vessel will be approximately six times greater. As real vessels are corrupted by noise, they will not perfectly overlap with the ideal model. So in the presence of noise the optimal scale is just a measure, where the structure of interest could have been best enhanced.

Choice of β_2: In general the value of β_2 depends on the strength of the noise and background structures in the image. It should be large in order to prevent enhancement of spurious low contrast data [5]. Based on the assumed ideal vessel model we will compute an upper bound for β_2 in the absence of noise. From eq. 5 it can be easily observed that the values of the filter answer $r^{\gamma-\mathrm{norm}}(\bar{\boldsymbol{x}}, t, \beta_1, \beta_2, \gamma)$ are bound within the interval $[0, 1]$. At $x = 0$, the filter answer of eq. 7 should be maximal for the optimal scale $t_{\mathrm{opt}} = t_0$ and $\gamma = \frac{3}{2}$; i.e the response $r^{\gamma-\mathrm{norm}}(\mathbf{0}, t_{\mathrm{opt}} = t_0, \beta_1, \beta_2, \frac{3}{2}) = 1 - \exp\left(-\frac{1}{8\pi\beta_2^2 t_0^{\frac{3}{2}}}\right) \stackrel{!}{=} 1$. We define a desired precision $\epsilon << 0$ for the exponential to be assumed equal to zero. We get therefore the upper bound for β_2

$$\beta_2 \leq \sqrt{-\frac{1}{8\pi \ln(\epsilon)}} \sqrt{t_0}^{\frac{3}{2}}. \tag{9}$$

This upper bound depends on the standard deviation of the assumed model $\sqrt{t_0}$. As a fixed value for β_2 is required for all considered scales, we get concrete values for β_2 by considering the maximal scale value. The bound given by eq 9 represents the part of β_2 which depends on the geometrical structure of the line model. It is to be understood as

an indication of the order of magnitude of β_2 in the ideal case. In real images β_2 should still be tuned heuristically, to count for the gray levels in the background at hand.
Choice of β_1: The value of β_1 should be small in order to distinguish between line-like and blob-like structures. If bifurcations or very tortuous vessels are not enhanced properly, increasing β_1 resolves that at the expense of also enhancing non-vessel background structures [5]. As $|\lambda_1(\bar{\boldsymbol{x}}, t)| < |\lambda_2(\bar{\boldsymbol{x}}, t)|$ and due to the symmetry of the exponential function we can compute the blobness based on the absolute values of the λ's. The values of ${\mathcal{R}_{\mathcal{B}}}^{\gamma-\mathrm{norm}}(\bar{\boldsymbol{x}}, t)$ are then bound between $[0, 1]$, It is one when the structure is a blob and it is near zero if the structure is a line or an edge. A value $\beta_1 = 0.33$ discards all blob similar structures. Greater values (≤ 1) are less discriminative, but more tolerant to deviations from the ideal model.

3 Discretization and Numerical Implementation

Two questions arise when we are given a discrete 2D image. First: How to get a discrete scale-space of the image? Second: How to discretize the scale parameter t?
Discrete Scale-Space: A straightforward discretization of eq 4 is accomplished by performing the *discrete convolution* of the image with the *discrete Gaussian kernel*, while keeping the scale parameter t continuous. The discretization of the Gaussian kernel can be performed in several ways. The most known are by directly computing the continuous Gaussian function at discrete locations (the *sampled Gaussian kernel*) or by integrating the continuous kernel over each pixel support region (the *integrated Gaussian kernel*). The sampled Gaussian kernel has the problem, that for small values of t the central coefficient of the sampled Gaussian can become very large and the sum of the corresponding filter coefficients will exceed one[4]. The integrated Gaussian kernel can be regarded as giving a more true approximation than the first method, especially at fine scales. The resulting approximation formula corresponds to discrete convolution with the kernel $g(n, t) = \int_{n-\frac{1}{2}}^{n+\frac{1}{2}} \frac{1}{\sqrt{2\pi t}} \exp^{-\frac{\xi^2}{2t}} d\xi$. This choice of filter coefficients is equivalent to the continuous formulation 4 if we let the continuous image be a piecewise constant function [4, 6]. The kernel coefficients for the Gaussian, and its derivatives are computed as given in[6]. The mask sizes are computed automatically depending on the given σ such that the approximation error is set to a certain ϵ_g. At borders the gray values are mirrored.
Discrete Scales: In practice we need to choose a certain number of scales that best approximate the characteristic parameters in the image at hand. The maximum and minimum values of $\sigma = \sqrt{t}$ should be determined on the basis of the width range of the vessels of interest. In [2] the minimum number of scale was automatically determined based on certain response specific criteria. The set of discrete scales σ_i is computed according to $\sigma_i = \sigma_l s^i$ width $s > 1$ a scaling factor, $i = 0, 1, \cdots, n-1$ and n the number of scales such that $\sigma_l s^{n-2} < \sigma_h \leq \sigma_l s^{n-1}$. It follows that

$$n < \frac{\ln(\frac{\sigma_h}{\sigma_l})}{\ln(s)} + 2 \leq n + 1 \tag{10}$$

We took the smallest nearest integer value of eq. 10 for n. We get thus a logarithmic progressing of scales and an automatic determination of their number.

4 Experiments

4.1 Experiments on Phantom Data

We generated a phantom image ($420 \times 420 \times 8$) containing line structures having Gaussian profiles of different widths: A vertical line with $\sigma_0 = 1$, a horizontal line with $\sigma_0 = 5$ and a circular structure with $\sigma_0 = 3$ and radius $r = 100$. (see fig. 1). The vertical line crosses the circle along its middle axis. The horizontal line is shifted to the bottom by 30 pixels. The positioning of the lines aims to show the behavior of the filter on straight line, curvilinear structure as well as at crossings or bifurcations.

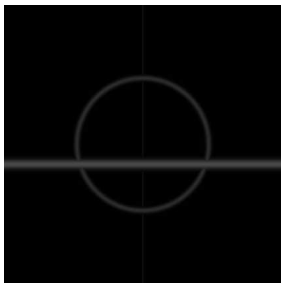

Fig. 1. Phantom image.

By taking the ideal Gaussian profile $I_0(\bar{\boldsymbol{x}})$ of sec. 2, lines with smaller width will be assigned brighter gray values. In real angiographic images the opposite behavior is rather observed. To simulate this phenomenon we inverted the proportionality with respect to σ. The underlying Gaussian profiles used for generating the phantom are $\frac{\sigma_0}{\sqrt{2\pi}}\exp\left(\frac{-x^2}{2\sigma_0^2}\right)$ for the straight lines and $\frac{\sigma_0}{\sqrt{2\pi}}\exp(-\frac{(r-\sqrt{x^2+y^2})^2}{2\sigma_0^2})$ for the circular profile. To be able to assess the enhancement effect we assigned a gray value of 15 to the maximum value of the line with the smallest width. Based on this, the gray level mapping function is linear. Background color was set to one. When two lines cross the maximal value in the overlapping area is taken.

We performed multiscale analysis with maximization of normalized responses. We used $\beta_1 = 0.33$, which is the most restrictive value. The maximal width in the image is $\sigma = 5$ and by choosing $\epsilon = 10^{-8}$ in eq. 9, we became a value of $\beta_2 = 0.52$. The normalization factor is $\gamma = 1.5$. We chose $\sigma_l = 1$, $\sigma_h = 5$. By setting the scaling factor of eq. 10 to $s = 1.5$ five scales were automatically computed $\sigma \in \{1, 1.5, 2.25, 3.375, 5.0625\}$. The results for filter 5 and normalized filter 1 are shown in figure 2. Tuning β_2 results in fig. 3.

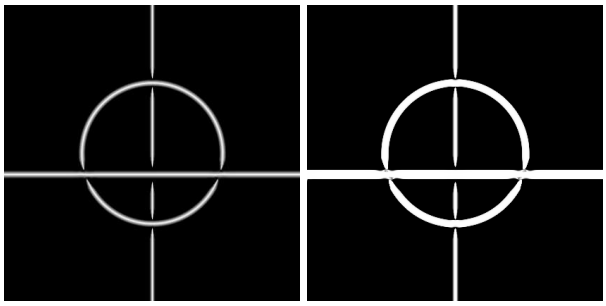

Fig. 2. Multiscale results with filter 5 (left) and filter 1 (right).$\beta_2 = 0.52$, $\beta_1 = 0.33$, $\gamma = 1.5$,$\sigma_l = 1$,$\sigma_h = 5$.

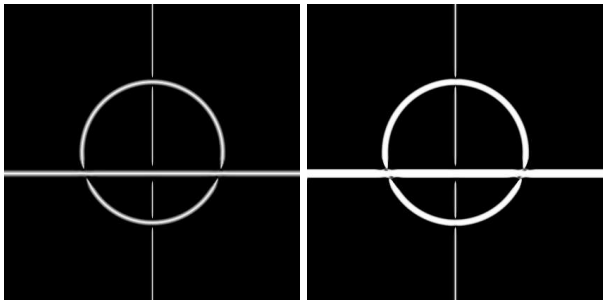

Fig. 3. Multiscale results with filter 5(left) and normalized Frangi filter 1(right). $\beta_2 = 2.0$.

The effect of both vessel enhancement filters can be quantitatively compared according to three factors: First which filter better increases the local contrast between vessel and background. Second which filter better preserves the original line width. And third which filter better enhances the centerlines of the vessels. Due to the symmetry of the phantom used we computed these values along one cross section for each of the three lines and excluded thus crossings since they do not have line properties. The local contrast was measured by the mean value of mean gray levels within the lines in the original and enhanced images. The width was computed by the mean value of the number of pixels whose gray levels are different from background. And the enhancement of the centerline was measured by computing the ratio of gray levels along the cross section of the lines and the gray value of the centerline. Tables 1 and 2 summarizes the quantitative results.

	image	**local contrast**	**width**
	original	21.025	15.66
$\beta_2 = 0.52$ Fig 2	normalized Frangi eq. 1	151.37	9.66
	extended filter eq. 5	77.467	9
$\beta_2 = 2.0$ Fig 3	normalized Frangi eq. 1	119.13	9
	extended filter eq. 5	69.321	8.66

Table 1. Quantitative comparison between normalized Frangi filter 1 and extended filter 5: Comparison of local contrast and preservation of line width. Mean values over three line sizes are reported

By observing figures 2 and 3 both filters show very week responses in regions where two lines cross, i.e. where no line properties are present. This appears as a discontinuity. Normalization of the filters leads to comparable values along different scales. Especially great scales become higher responses. Both filters enhance the local contrast compared with the original one (table 1). The extended filter 5 results in lower local contrast since the additional edge indicator term in eq 3 is always within $[0, 1]$. The behavior of both filters is comparable with respect to preservation of the width of lines. It is basically reduced, especially for wide lines (see Also curves in table 2). This may be due to the

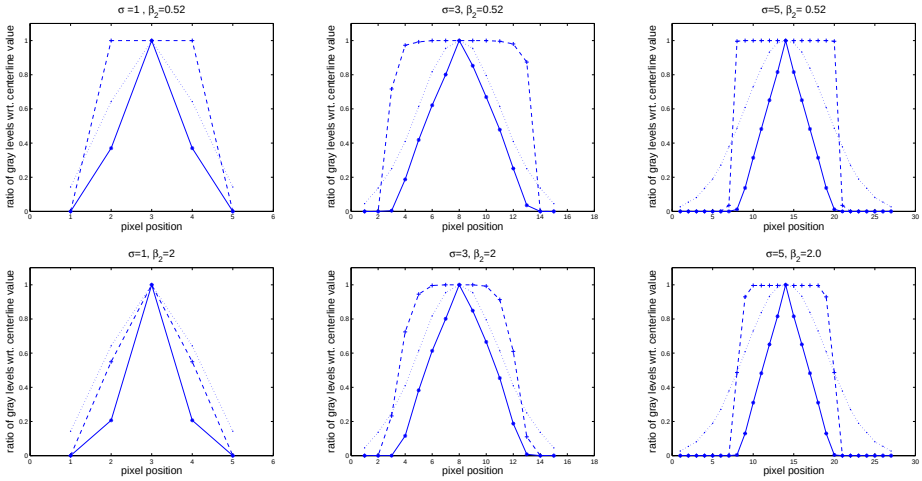

Table 2. Quantitative comparison between normalized Frangi filter 1 and extended filter 5: comparison of centerline enhancement. Top $\beta_2 = 0.52$; from left to right $\sigma = 1, 3, 5$ respectively. Bottom $\beta_2 = 2.0$; from left to right $\sigma = 1, 3, 5$ respectively. Original line: dot line, Frangi filter: dashed line, extended filter: continuous line. Cross section values are reported

weak slope of wider lines. The gain from adding the edge indicator becomes clear by observing the curves of enhancement of the centerlines in table 2. The normalized filter 1 enhances the borders of the lines without particularly enhancing centerlines. The values accorded to the centerlines by filter 5 are more discriminative and facilitates further processing such as centerline extraction. Increasing β_2 increases the discriminative power –especially of the normalized Frangi filter–, decreases the local contrast and tends to reduce the resulting width of lines.

4.2 Experiments on Real Data

We apply vessel enhancement on real coronary angiograms ($512 \times 512 \times 8$) captured by a monoplane Siemens AXIOM Artis system (rotational angiography). The images have a black border, which is not considered in treatment. We set $\beta_1 = 0.5$, $\gamma = 1.5$ and $s = 1.5$. By choosing $\sigma_h = 4$ we become a value of $\beta_2 = 0.38$. For $\sigma_l = 1$ and $\sigma_h = 4$ five scales are automatically computed $\sigma \in \{1, 1.5, 2.25, 3.375, 5.0625\}$. Fig. 4 shows a typical image, its corresponding preprocessed images with both filters 5 and 1. Figure 5 shows two preprocessed images with variation of β_2 leading to less Background noise.

With the theoretical discussed values for the free parameters the filters 5 and 1 were able to enhance the interesting structure and also a lot of Background. Increasing β_2 eliminates background structures (fig. 5) and better reflects the real widths of vessels, as it was already observed in the phantom image. With real images we observe the poor discriminative performance of the responses of the Frangi filter 1 between centerlines and borders. Another consequence of non-distinction between edges and line structures

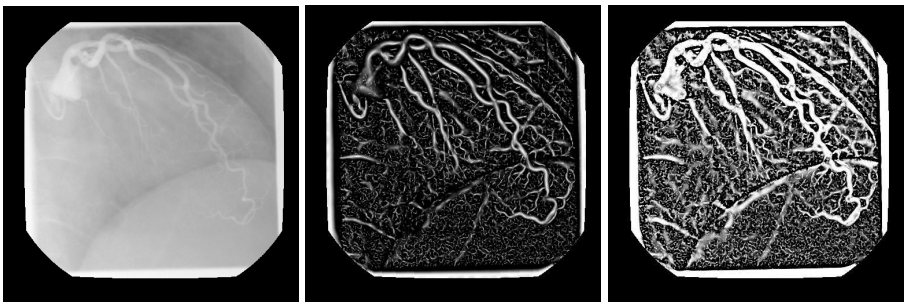

Fig. 4. From left to right: original image, filter 5, normalized filter 1 with same parameters

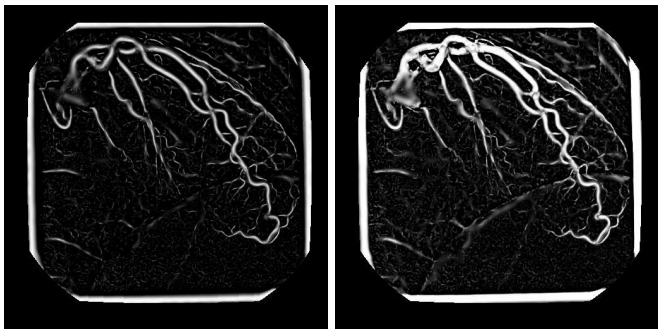

Fig. 5. Less Background noise. Left: filter 5 with $\beta_2 = 1.0$. Right: filter 1 with $\beta_2 = 1.0$

is the enhancement of the diaphragm with the Frangi filter (fig. 4, right); as it is considered as an edge.

Both filters were able to recognize fine vessels and also fine ramifications, thanks to the multi-scale response. Problems arise with very tortuous vessels and at bifurcations or crossings, where the eigenvalues have comparable values and so no line properties can be detected (increasing β_1 does not ameliorate the result). Fig. 6 show magnified regions of different images where this effect is observed. At this magnified scale the improvement reached by integrating the edge indicator is again enhanced by the smooth responses and preservation of the vessel trajectory.

5 Conclusion

In this paper we extended the Frangi filter [1] for 2D-vessel enhancement to better differentiate between edges and line structures. We integrated the normalization of Gaussian derivatives in the filter response. We performed an optimal scale selection by assuming an ideal model and gave theoretical values or bounds for the filter free parameters. We presented experiments on phantom data to objectively and quantitatively compare and judge the filters in the ideal case. The performed extension lead mainly to stronger discrimination of the centerlines after enhancement. Experiments on real

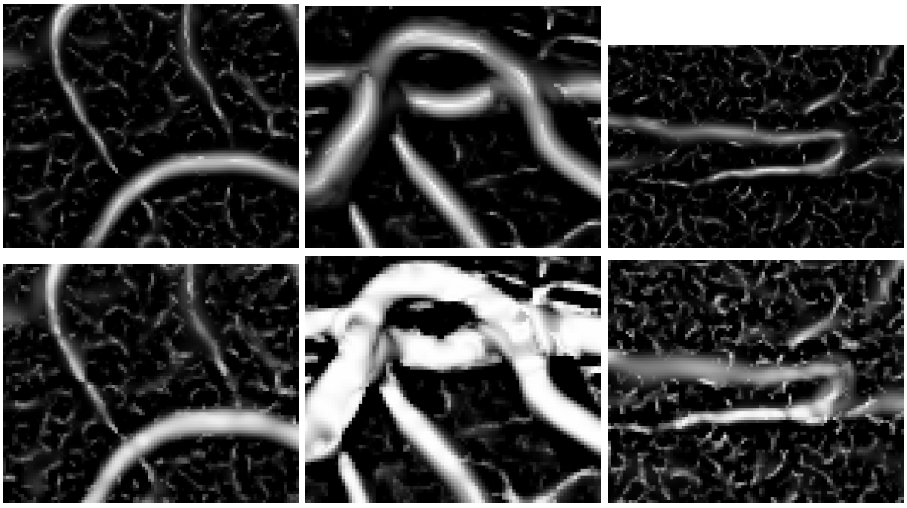

Fig. 6. Magnification of bifurcations, crossings and a tortuous vessel. Top: results of filter 5. Bottom: results of normalized filter 1

angiographic data showed this improvement under real conditions. This contribution is to be understood as preprocessing for further steps such as centerline extraction or temporal tracking of vessels for 3D heart motion recovery [7].

References

1. Frangi, A., Niessen, W.J., Hoogeveen, R.M., van Walsum, T., Viergever, M.A.: Model-based quantitation of 3-d magnetic resonance angiographic images. TMI **18**(10) (10 1999) 946–956
2. Sato, Y., Nakajima, S., Shiraga, N., Atsumi, H., Yoshida, S., Koller, T., Gerig, G., Kikinis, R.: 3d multi-scale line filter for segmentation and visialization of curvilinear structures in medical images. In: IEEE Medical Image Analysis. Volume 2. (6 1998) 143–168
3. Lorenz, C., Carlsen, I.C., Buzug, T.M., Fassnacht, C., Weese, J.: A multi-scale line filter with automatic scale selection based on the hessian matrix for medical image segmentation. In: Proc. of the First Int. Conf. on Scale-Space Theory in Computer Vision. (1997) 152–163
4. Lindeberg, T.: Scale-space for discrete signals. IEEE Transactions of Pattern Analysis and Machine Intelligence **12**(3) (1990) 234–254
5. Schrijver, M., Slump, C.H.: Automatic segmentation of the coronary artery tree in angiographic projections. In: Proc. Program for Research on Integrated Systems and Circuits (PRORISC). (2000)
6. Steger, C.: An unbiased detector of curvilinear structures. PAMI **20**(2) (1998) 113–125
7. Bouattour, S., Arndt, R., Paulus, D.: 4d reconstruction of coronary arteries from monoplane angiograms. In: Computer Analysis of Images and Patterns. 11th International Conference CAIP 2005, Versailles, France, Springer, Berlin, Heidelberg, New York (2005)